An Introduction to Gravitational Collapse to Black Holes

Luciano Rezzolla*

SISSA, International School for Advanced Studies and INFN, Trieste, Italy

Department of Physics and Astronomy, Louisiana State University, Baton Rouge, LA 70803 USA

---

*`www.sissa.it/~rezzolla`

1 Introduction

The numerical investigation of gravitational collapse of rotating stellar configurations lead-ing to black hole formation is a long standing problem in numerical relativity. However, it is through numerical simulations in general relativity that one can hope to improve our knowledge of fundamental aspects of Einstein's theory such as the cosmic censorship hypothesis and black hole no-hair theorems, along with that of current open issues in rel-ativistic astrophysics research, such as the mechanism responsible for gamma-ray bursts. Furthermore, numerical simulations of stellar gravitational collapse to black holes pro-vide a unique means of computing the gravitational waveforms emitted in such events, believed to be among the most important sources of detectable gravitational radiation.

The modelling of black hole spacetimes with collapsing matter-sources in multidimen-

sions is one of the <u>most formidable efforts</u> of numerical relativity. This is due, on one hand, to the nonlinear properties of the equations to be integrated (the Einstein equations coupled to the hydrodynamics equations), and, on the other hand, to the vast computational resources needed in three-dimensional (3D) evolutions.

I will give a very brief overview of this research area, discussing in particular

- why <u>black holes</u> may be final state of compact stars

- toy-model: collapse of a dust sphere to a <u>black hole</u> (Oppenheimer-Snyder)

- dynamics of trapped surfaces

- non-spherical collapse to <u>black holes</u>

Hereafter, I will assume the reader is familiar with the foundations of General Relativity, use a spacelike signature $(-, +, +, +)$ and a system of units in which $c = G = M_\odot = 1$.

2 Compact Stars and Black Holes

Within a more realistic astrophysical context, any discussion on gravitational collapse to black holes would necessarily start from considering the existence of the "progenitors", i.e. of stars that during their evolution would meet conditions in which the pressure support can no longer balance the gravitational attraction. However, I will not do this here and, rather, by-pass the problem assuming that I can construct a spherical stellar model which will not be able to avoid to collapse to a black hole.

All you need to do to convince yourself that this scenario is at least plausible if not realistic[1] is to consider the simplest possible example: i.e. a spherically-symmetric, uniform density, perfect-fluid star. Before we look into why the gravitational collapse may be unavoidable in this case, let us construct such a star which will be described by a stress-

---

[1]In a constant density star the speed of sound is infinite and clearly unphysical. However, the interior of neutron stars the density is nearly uniform.

energy tensor of the type

$$T^{\mu\nu} = (\rho + p)u^\mu u^\nu + pg^{\mu\nu}, \tag{1}$$

where ρ, u^μ and p are the total mass-energy density, the fluid 4-velocity and the (isotropic)

pressure, respectively.

The stellar configuration will therefore be a solution of the hydrodynamics equations

for the conservation of energy-momentum

$$\nabla_\alpha T^{\alpha\beta} = 0. \tag{2}$$

and of baryon number $n \equiv \rho_*/m_0$

$$\nabla_\alpha(nu^\alpha) = 0. \tag{3}$$

where m_0 is the mass of the particles composing the fluid (I am assuming they are of one

type only) and ρ_* the rest-mass density. In eqs. (2) and (3), the operator ∇ represents the

covariant derivative with respect to the spherically symmetric line-element

$$ds^2 = -e^{2\Phi}dt^2 + e^{2\Lambda}dr^2 + r^2 d\Omega^2. \tag{4}$$

where $d\Omega^2 = d\theta^2 + \sin^2\theta d\phi^2$. Projecting now eq. (2) in the direction orthogonal to the fluid 4-velocity through the projector operator

$$P^{\alpha\beta} = u^\alpha u^\beta + g^{\alpha\beta}. \tag{5}$$

we obtain the general relativistic Euler equations

$$(p + \rho)a_\mu = -P_\mu{}^\beta p_{,\beta}, \tag{6}$$

where $a_\mu \equiv u_{\mu;\beta}u^\beta$ is the fluid 4-acceleration. Once recast in form (6), the comparison with the corresponding Euler equations for a fluid with 3-velocity v^i in a Newtonian potential Φ_{Newt}

$$\rho(\partial_t v^i + v^j \partial_j v^i) = -\partial^i p - \partial^i \Phi_{\text{Newt}}, \tag{7}$$

is rather transparent. Imposing the conditions of stationarity and spherical symmetry, the only non-trivial Euler equation reduces to

$$(p + \rho)\frac{d\Phi}{dr} = -\frac{dp}{dr} \tag{8}$$

where Φ is there a metric potential and is clearly related to the corresponding Newtonian gravitational potential Φ_{Newt}. Next, we consider the Einstein field equations $G_{\alpha\beta} = 8\pi T_{\alpha\beta}$ and introduce a re-parametrization of the radial metric function introducing the function

$$m(r) \equiv \frac{1}{2}r(1 - e^{-2\Lambda}), \tag{9}$$

so that

$$g_{rr} \equiv e^{2\Lambda} = \left(1 - \frac{2m(r)}{r}\right)^{-1}. \tag{10}$$

Indicating with a $'$ the radial derivative, the non-zero components of the Einstein tensor

are

$$G_{00} = \frac{e^{2\Phi}}{r}[r(1 - e^{-2\Lambda})]', \quad G_{rr} = -\frac{e^{2\Lambda}}{r}(1 - e^{-2\Lambda}) + \frac{2}{r}\Phi', \quad (11)$$

$$G_{\theta\theta} = r^2 e^{-2\Lambda}\left[\Phi'' - (\Phi')^2 + \frac{\Phi'}{r} - \Phi'\Lambda' - \frac{\Lambda'}{r}\right], \quad G_{\phi\phi} = G_{\theta\theta}\sin^2\theta. \quad (12)$$

so that the Einstein equations become

$$\frac{dm(r)}{dr} = 4\pi r^2 \rho, \quad (13)$$

$$\frac{dp}{dr} = -\frac{(p + \rho)(m + 4\pi r^3 p)}{r(r - 2m)}. \quad (14)$$

Eqs. (8), (13), (14) together with an equation of state relating p and ρ [i.e. $p = p(\rho)$] are known as the Tolmann, Oppenheimer, Volkoff (TOV) equations and their solutions requires, in general, a numerical integration. Fortunately, in the case of a spherically-

symmetric, uniform-density star, analytic expressions are available.

Recalling that Birkhoff's theorem guarantees that the exterior spacetime will be the Schwarzschild one, we easily deduce that the metric functions will be given by

$$
g_{rr} = \begin{cases} \left(1 - \dfrac{2}{r}\dfrac{4\pi r^3}{3}\rho_0\right)^{-1} & \text{for } r \leq R \text{ (interior)}, \\[2ex] \left(1 - \dfrac{2M}{r}\right)^{-1} & \text{for } r > R \text{ (Schwarzschild)}, \end{cases} \tag{15}
$$

and

$$
\sqrt{-g_{tt}} = e^{\Phi} = \begin{cases} \dfrac{3}{2}\left(1 - \dfrac{2M}{R}\right)^{1/2} - \dfrac{1}{2}\left(1 - \dfrac{2Mr^2}{R^3}\right)^{1/2} & \text{for } r \leq R \text{ (interior)}, \\[2ex] \left(1 - \dfrac{2M}{r}\right)^{1/2} & \text{for } r > R \text{ (Schwarzschild)}, \end{cases}
$$

where M is the "gravitational mass" of the star

$$
M = \int_0^R 4\pi r^2 \rho_0 dr = \frac{4\pi}{3}R^3\rho_0, \tag{16}
$$

so that

$$\rho_0 = \frac{3M}{4\pi R^3}, \tag{17}$$

R its radius and ρ_0 the average density. Note that although the density is uniform within the star, the pressure is not and is given by

$$p = p(r) = \rho_0 \frac{(1 - 2Mr^2/R^3)^{1/2} - (1 - 2M/R)^{1/2}}{3(1 - 2M/R)^{1/2} - (1 - 2Mr^2/R^3)^{1/2}}, \tag{18}$$

so that the radius can be calculated explicitly from the values of ρ_0 and the central pressure

$$p_c \equiv p(r = 0) = \rho_0 \frac{1 - (1 - 2M/R)^{1/2}}{3(1 - 2M/R)^{1/2} - 1}, \tag{19}$$

as the radial position at which $p = 0$

$$R = \frac{3}{8\pi\rho_0} \left[1 - \frac{(\rho_0 + p_c)^2}{(\rho_0 + 3p_c)^2} \right]. \tag{20}$$

Overall, the uniform-density solution depends on a single parameter ρ_0, but has an important limit in the compactness M/R. In particular, eq. (19) indicates that $p_c \to \infty$ for

$M/R \to 4/9$ so that infinite pressures are necessary to support a star with a radius smaller than $9/8$ of the Schwarzschild radius $R_S \equiv 2M$. As a result, *should a star reach such compactnesses, its final fate can only be that of a black hole* (This is also known as "Buchdal's theorem" and applies also for realistic equations of state.).

3 Collapse of a dust sphere to a black hole

So far we have concentrated on stationary configurations but the gravitational collapse is clearly a dynamical process involving considerable portions of spacetime. Also in this case, it is useful to start studying a simplified scenario as the one offered by the collapse of a star composed of uniform-density pressurless dust. This is also known as the Oppenheimer-Snyder (OS) collapse. In this case, in fact, the fluid motion is particularly simple (i.e. it is that of collisionless particles having a collective motion in the same direction) and the spherical symmetry (via the Birkhoff's theorem) guarantees that the only portion of the spacetime that is undergoing an effective evolution is the stellar interior one, since the exterior always remains that of a Schwarzschild solution (albeit with a dynamical boundary).

Before looking at the details of the dynamics it is useful to consider the set of equations, both Einstein and hydrodynamical, that describe the process; as we will see, these equations are well known also in a different (cosmological) contest.

We start considering a spherically symmetric, diagonal line element [2] of the form

$$ds^2 = -a^2 dt^2 + b^2 dr^2 + R^2 d\Omega^2. \tag{21}$$

where a and b are functions of (r, t). Here, R is a circumferential radial coordinate since the proper circumference is calculated simply as

$$\mathcal{C} = \int_{r,\ \theta\ =\ \text{const.}} \sqrt{ds^2} = \int \sqrt{g_{\phi\phi}} d\phi = 2\pi R. \tag{22}$$

Adopting a set of comoving coordinates, the fluid 4-velocity is $u^\alpha = (u^0, 0, 0, 0)$, and since

---

[2] In spherical symmetry we can always to this.

$u^\alpha u_\alpha = -1$, we have that

$$u^\alpha = (a^{-1}, 0, 0, 0), \qquad u_\alpha = (-a, 0, 0, 0). \qquad (23)$$

To cast the hydrodynamic equations in a form that resembles the Newtonian one, it is better to introduce differential operators that measure variations with respect to the proper distance. In general

$$\frac{\partial}{\partial(\text{proper } x^\beta \text{ coordinate})} = \frac{\partial}{\sqrt{g_{\alpha\beta}}\partial x^\beta}, \qquad (24)$$

$$D_t = \text{proper time derivative} \equiv \frac{1}{a}\partial_t, \qquad (25)$$

$$D_r = \text{proper radius derivative} \equiv \frac{1}{b}\partial_r. \qquad (26)$$

As a result, we can introduce the quantities

$$u \equiv D_t R = \frac{1}{a} \partial_t R, \qquad \Gamma \equiv D_r R = \frac{1}{b} \partial_r R, \qquad (27)$$

so that u is the radial component of a 4-velocity in a coordinate system that has R as the radial, while Γ measures the variation of the circumferential radius with respect to the radial coordinate. Within this framework, the full set of hydrodynamics and field

equations is then given by

$$\frac{D_t \rho}{(\rho + p)} = \frac{D_t \rho_0}{\rho_0}, \qquad \text{(conservation of energy)}, \qquad (28)$$

$$\frac{D_t \rho_0}{\rho_0} = -\frac{1}{R^2} \partial_R(uR^2), \qquad \text{(conservation of baryon number)}, \qquad (29)$$

$$D_t u = -\frac{\Gamma}{\rho + p} D_r p - \frac{m}{R^2} - 4\pi p R, \quad \text{(conservation of momentum)}. \qquad (30)$$

$$D_t \Gamma = -\frac{u}{\rho + p} D_r p, \qquad\qquad D_t m = -4\pi R^2 u \rho. \qquad (31)$$

$$\Gamma = 1 + u^2 - \frac{2m}{R}. \qquad (32)$$

Note that eq. (32) indicates how Γ is the general relativistic analogue of the Lorentz factor

in special relativity ($\Gamma = 1$ in Newtonian physics). Eqs. (28) − (32), together with an

equation of state, represent the set of equations to be solved to compute the evolution of the interior spacetime of a spherical collapse.

Note also that since the dust particles will be collisionless and all having the same radial motion, $p = 0$ and this simplifies the above set of equations considerably. Also, since the rest-mass is conserved during the collapse we can introduce new variable that labels different shells with the rest-mass they contain, i.e.

$$\mu(r) = \int 4\pi R^2 \rho_* b \, dr. \tag{33}$$

where ρ_* is the rest-mass density. Clearly, this parametrization is valid as long as each shell does not interact with the neighbouring ones, i.e. there is no shell-crossing.

Let us now consider in detail the consequences of the assumption that the fluid is *homogeneous*, i.e. $D_r p = 0 = D_r \rho$. In this case, the first of eqs. (31) reduces to $D_t \Gamma = 0$, so that

$\Gamma = \Gamma(\mu)$ only and

$$m = \int_0^{R_0} 4\pi R^2 \rho \, dR = \frac{4\pi}{3} R_0^3 \rho. \tag{34}$$

Let us now adopt a "comoving-observer gauge", i.e. a gauge in which the time coordinate is the proper time on a line $dx^i = 0$ and such that $g_{00} = a = 1$ or, equivalently, $D_t = \partial_t$. Furthermore, because of the homogeneity at any point, we can decompose $R = R(\mu, t)$ as $R = F(t)\widetilde{R}(\mu)$, so that

$$\dot{R} \equiv \partial_t R = u = \dot{F}\widetilde{R} = \frac{\dot{F}}{F}R, \tag{35}$$

and the Einstein eq. (32) becomes

$$\Gamma^2 = 1 + u^2 - \frac{2m}{R} = 1 + R^2 \left[\left(\frac{\dot{F}}{F} \right)^2 - \frac{8\pi\rho}{3} \right] = 1 - \kappa \frac{R^2(\mu, t)}{S^2(t)}, \tag{36}$$

where $\kappa = 0, \pm 1$ accounts for the sign of the term in square brackets and S is a function of time only and just a shorthand for what contained in the square brackets. Because of the

decomposition of R, the ratio $\widetilde{R}/S$ is a function of r only and thus we can simply write

$$\Gamma^2 = 1 - \kappa r^2, \tag{37}$$

so that the line element (21) becomes

$$ds^2 = -a^2 dt^2 + b^2 dr^2 + R^2 d\Omega^2 = -dt^2 + S^2(t) \left[\frac{dr^2}{1 - \kappa r^2} + r^2 d\Omega^2 \right]. \tag{38}$$

Clearly, the line element (38) is the metric of a <u>Friedmann-Robertson-Walker</u> cosmological solution where the function S (i.e. the conformal factor of the spatial part of the metric) is simply the "scale factor". Similarly, it will not be surprising that when expressed in this metric, the hydrodynamic and Einstein equations will essentially reduce to the Friedmann

equations

$$\ddot{S} = -\frac{4\pi}{3}(p + \rho)S, \tag{39}$$

$$\dot{S}^2 - \frac{8\pi}{3}\rho S^2 = -\kappa. \tag{40}$$

Stated differently, the spatial part of the line element (38) describes geometries with different constant curvatures (i.e the curvature is the same everywhere but it is not constant in time), with the different geometries being selected by the values of the coefficient κ.

Stated differently, *in spherical symmetry, the dynamical spacetime of a collapsing (expanding) region occupied by homogeneous matter is a Friedmann-Robertson-Walker (FRW)-Universe.*

Cosmologically, there are three possible solutions according to the value of κ and thus on the constant curvature ($\kappa = -1$, curved open Universe; $\kappa = 0$: flat Universe, $\kappa = 1$;

curved closed Universe). Clearly, the relevant solution in the context of an OS collapse is the one with positive constant curvature (i.e. $\kappa = 1$) in which case the line element can be expressed in terms of comoving hyperspherical coordinates (χ, θ, ϕ)

$$ds^2 = -d\tau^2 + S(\tau)[d\chi^2 + \sin^2\chi d\Omega^2] \tag{41}$$

where $\chi = \sin^{-1} r$.

There is an important difference between the FRW Universe and the spacetime of an OS collapse since in the latter case not all of the spacetime is occupied by matter (the dust sphere has initially a finite radial size R_0) and the vacuum portion (i.e. for $R > R_0$) will be described by a Schwarzschild spacetime. The matching between the two portions can be done at the surface of the star my requiring the continuity of the proper circumference

$$\mathcal{C}_{\text{Schw.}} = \int \sqrt{g_{\phi\phi}}d\phi = 2\pi R_0 = \mathcal{C}_{\text{FRW}} = 2\pi S \sin \chi_0. \tag{42}$$

Since (42) must hold at all times, we have that

$$R_0 = S \sin \chi_0. \tag{43}$$

Let us now consider the equations of motion in the collapsing portion of the spacetime. In this case, eq. (31), reduces to $D_t m = -4\pi R^2 u p = 0$, thus implying that m is not a function of time but of radius only, i.e. $m = m(\mu)$ as it should be in the absence of shocks. Similarly, eq. (30) reduces to

$$D_t u = -m/R^2 \tag{44}$$

which is essentially the geodetic equation. The trajectory of any shell can therefore be obtained through a time integration of (44) and is given by

$$\dot{R} \equiv \frac{dR}{d\tau} = D_t R = \left(\frac{2m}{R} - \frac{2m}{R_0} \right)^{1/2}. \tag{45}$$

In other words, a shell of dust will go from R_0 to $R = 0$ in a finite proper time

$$\tau = \frac{\pi}{2} R_0 \left(\frac{R_0}{2M} \right)^{1/2}. \tag{46}$$

Note that this time will be the same for all initial radial positions R; this is a trivial conse-

quence of the uniformity in density, for which the ratio $R^3/m(R) = \text{const.}$.
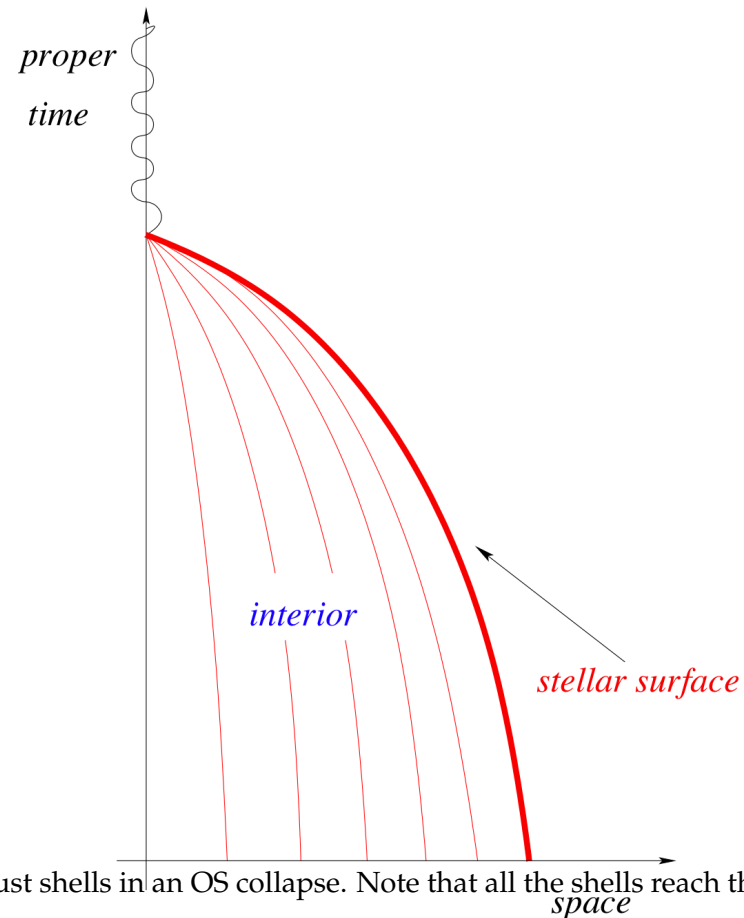
Figure 1: Schematic worldlines of dust shells in an OS collapse. Note that all the shells reach the singularity at the same proper time.

A schematic diagram showing the worldlines of different radial shells in an OS collapse is shown in Fig. 1. Note they all reach the singularity at the same proper-time $\tau = \frac{\pi}{2} R_0 \left(\frac{R_0}{2M} \right)^{1/2}$.

Once expressed in the coordinate system (41) and after introducing the $\eta \in [0, \pi]$ is the "cycloid parameter", the equations of motion take the simpler form

$$R = \frac{R_0}{2}(1 + \cos\eta), \qquad S(\eta(\tau)) = \frac{S_m}{2}(1 + \cos\eta), \qquad \tau = \frac{S_m}{2}(\eta + \sin\eta), \qquad (47)$$

where η is essentially playing the role of a time coordinate ($\eta = 0$ at the beginning of collapse and $\eta = \pi$ at the end) and is defined as $d\eta = d\tau/S$.

Using now eqs (47) and the condition (42) one finds that

$$S_m = \left(\frac{R_0^3}{2M}\right)^{1/2}, \qquad \chi_0 = \sin^{-1}\left(\frac{2M}{R_0}\right)^{1/2}. \qquad (48)$$

Particularly interesting is to calculate the proper time τ at which a shell initially at R_0 reaches $R = 2M$. This can be computed from (47) and is given by

$$\tau_{2M} = \left(\frac{R_0^3}{2M}\right)^{1/2}(\eta_{2M} + \sin\eta_{2M}), \qquad (49)$$

where $\eta_{2M} \equiv \cos^{-1}(4M/R_0 - 1)$. These expressions will be useful in the following Section, when I will discuss what happens to outgoing photons as the collapse proceeds and that may never reach null infinity.

4 Collapse of a dust sphere to a black hole: Trapped Surfaces

Assuming the cosmic censorship to hold (see ref. [1]), the end-result of the spherical collapse will be a Schwarschild black hole, the physical singularity will covered by an *event horizon*, a null surface that photons cannot leave. However, the Schwarzschild solution will be reached only asymptotically and is interesting to ask how the event horizon is formed during collapse; in practice we need to study the trajectory of the outermost outgoing photon that was not able to reach null infinity. Similarly, we can calculate where, at each instant during the collapse, the last outgoing photon will be sent and reach null infinity. This surface will mark the outermost trapped surface, i.e. the *apparent horizon* and by definition will always be contained within the event horizon.

Let's us consider therefore the worldline of an *outgoing radial photon*. In this case, $ds^2 =$

$0 = d\theta = d\phi$ and the line element (41) then yields the curves

$$\frac{d\chi}{d\tau} = \pm\frac{1}{S(\tau)} \,, \tag{50}$$

Using now the cycloid parameter η [cf. eqs (47)], it is easy to show that these photons propagate along straight lines in a (χ, η) plane

$$\frac{d\chi}{d\eta} = \pm 1, \tag{51}$$

or, stated differently, follow curves of the type

$$\chi = \chi_e \pm (\eta - \eta_e), \tag{52}$$

where χ_e and η_e and the "place" and "time" of emission, respectively. A swarm of outgoing photons will be *trapped* if their proper area will not grow in time, i.e. iff

$$\frac{d\mathcal{A}}{d\eta} \leq 0, \tag{53}$$

where $\mathcal{A} \equiv \int \sqrt{g_{\theta\theta} g_{\phi\phi}} d\theta d\phi$. Writing out the condition (53) explicitly yields

$$\eta_e \geq \pi - 2\chi_e, \tag{54}$$

which indicates that any outgoing photon emitted at a position χ_e and at a time η_e will be able to propagate out if and only if η_e is smaller that $\pi - 2\chi_e$ (i.e. a region in a (χ, η) plane).

Out of all the possible trapped surfaces, the most important is certainly the outermost one since it will discriminate between the photon that will propagate to null infinity from the one that will be trapped. Such a surface selects the apparent horizon and since $\chi_e \leq \chi_0$ (you must emit from within star) it is simply expressed as

$$\eta_{\mathrm{ah}} = \pi - 2\chi_0 = 2 \cos^{-1} \left(\frac{2M}{R_0} \right)^{1/2}, \tag{55}$$

where we have used expression (48) to derive the last term in (55).

It is now natural to ask: *when does the apparent horizon first form and where is it*

located? Luckily, answering these questions in the case of an OS collapse is particularly simple and reveals that the *apparent horizons first forms when the stellar surface crosses $R = 2M$*. Note that this is true only in the OS collapse.

Finally, we consider the evolution of the <u>event horizon</u> which is defined as the surface for which the equality in condition (53) holds. Using the constraint that the event horizon is always outside or coincides with the apparent horizon, we can set $\chi_{\mathrm{eh}} = \chi_{\mathrm{ah}}$ when $\eta = \eta_{\mathrm{ah}}$, the worldline for the event horizon is given by

$$\chi_{\mathrm{eh}} = \chi_0 + (\eta - \eta_{\mathrm{ah}}), \tag{56}$$

for $\eta \leq \eta_{\mathrm{ah}}$. Using now the circumferential radial coordinate we can write that

$$R_{\mathrm{eh}} = \frac{1}{2} \left(\frac{R_0^3}{2M} \right)^{1/2} (1 + \cos \eta) \sin(\chi_0 + \eta - \eta_{\mathrm{ah}}). \tag{57}$$

An important property to deduce from (57) is that the event horizon starts from a zero

radius and then progressively grows to reach $R = 2M$; this is to be contrasted with what

happens for the apparent horizon that is first formed with a nonzero radial size.
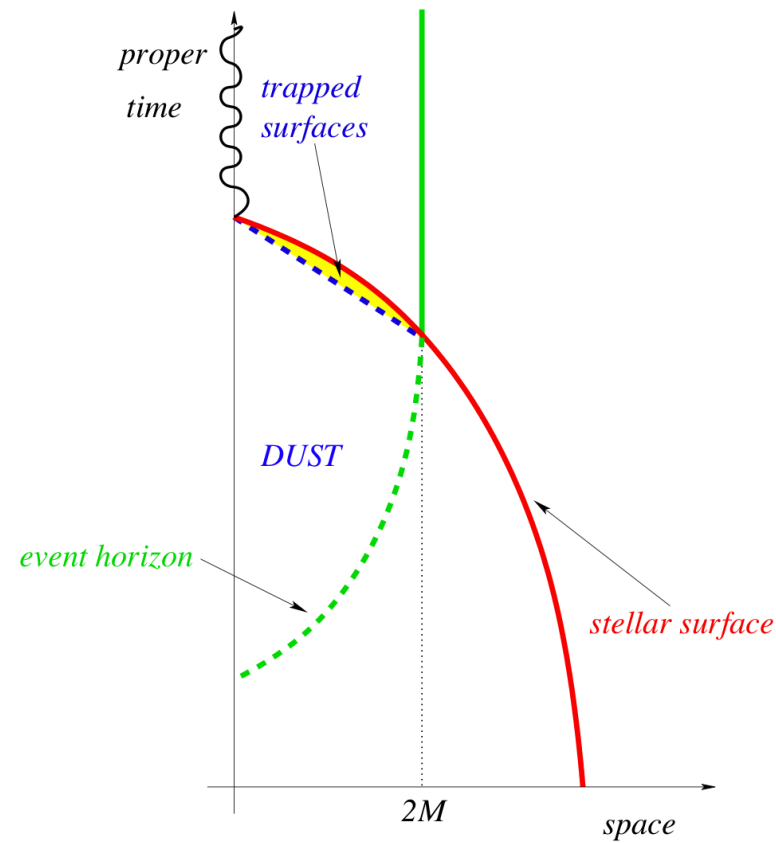
Figure 2: Schematic evolution of the relevant surfaces in the collapse of dust sphere.

The dynamics of the trapped surfaces is summarized in Fig. 2. Note that the event horizon grows from a zero size well before the apparent horizon is formed.

Much of what learnt about the dynamics of trapped in the OS collapse continues to hold also in the case of the collapse of a perfect fluid, which offers two two main differences with the respect to the case of dust. The first difference is present already in spherical symmetry and is that the apparent horizon is not produced at the time the stellar surface reaches $R = 2M$ but can, because of the fluid compression, be formed also earlier.
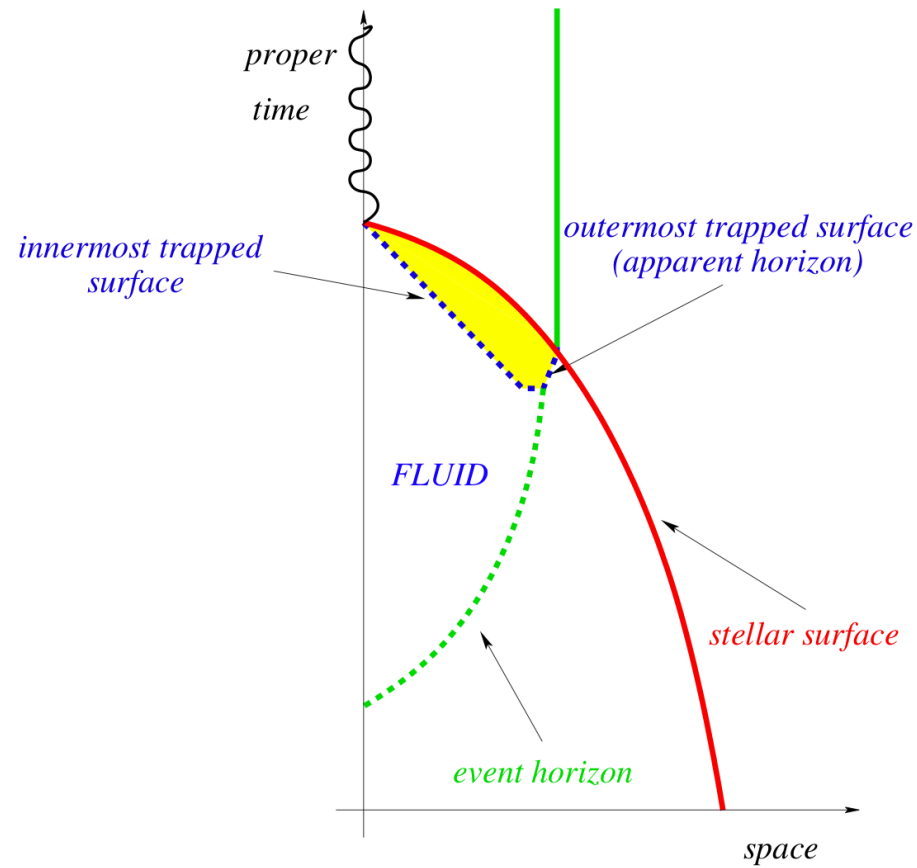
Figure 3: Schematic evolution of the relevant surfaces in the collapse of dust sphere.

The dynamics of the trapped surfaces is summarized in Fig. 3. Note that the apparent

horizon is formed after the event horizon but not when the stellar surface crosses $R = 2M$

5 Non-spherical Fluid Collapse

Recently, we have performed calculations in 3D and Cartesian coordinates of realistic initial data consisting of rapidly rotating neutron stars collapsing to Kerr black holes (Baiotti et al. (2004)). The initial stellar models were modelled as relativistic polytropes which are either secularly or dynamically unstable and with angular velocities which range from slow rotation to the mass-shedding limit. The study involved not only the dynamics of the matter, but also that of the trapped surfaces, *i.e.* of both the apparent and event horizons formed during the collapse. The use of these surfaces allows for a precise measurement of the black hole mass and spin. The dynamics of the collapsing matter is strongly influenced by the initial angular momentum and, for initial models with high angular velocities, the collapse can lead to the formation of an unstable disc in differential rotation.

6 A Crash-Course in Numerical Relativity

6.1 Einstein Equations

The Einstein equations written in the coordinate invariant form

$$G_{\mu\nu} = R_{\mu\nu} - \tfrac{1}{2}R = 8\pi T_{\mu\nu}$$

are a coupled system of 10 differential equations.

- *Locally* there exists a coordinate system where the speed of light is constant

- All physics is invariant under coordinate transformations

- For vacuum spacetimes $T_{\mu\nu}$ vanishes; not what we are interested in

- Space and time are fully mixed and time is on equal footings as space

- In numerical relativity some coordinate system must be introduced.

6.2 Covering a whole spacetime

The $3+1$ Cauchy form is natural for some situations. But the coordinate system chosen is unlikely to cover the whole spacetime. Other formulations can be chosen, such as the *characteristic* or *conformal* decompositions.

Cauchy   Characteristic   "Conformal"
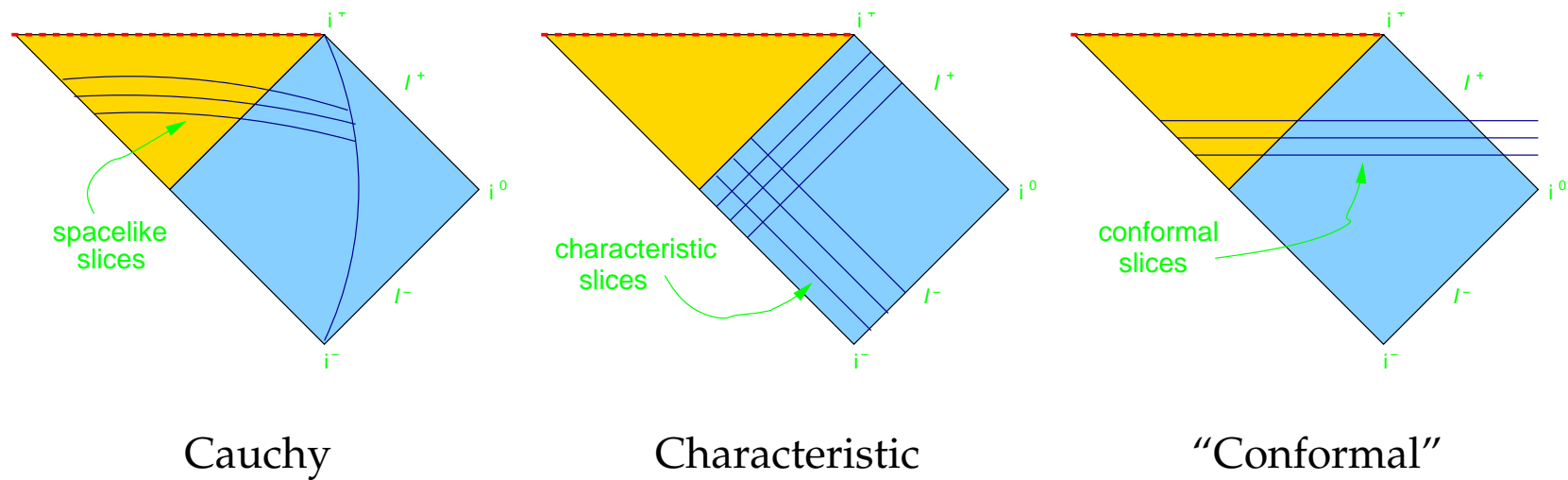
Each method has its advantages and disadvantages but we (as most of the groups in numerical relativity) use and restrict our attention to a $3+1$ Cauchy approach (Figs. by D. Pollney).

6.3   3+1 decomposition

A decomposition of spacetime in "space" (3) and "time" (1) was proposed by Arnowitt-Deser-Misner (1962). In practice, the idea is to split the 4-metric as

$$
\begin{bmatrix} g_{00} & g_{0b} \\[2mm] g_{a0} & g_{ab} \end{bmatrix} = \begin{bmatrix} -\alpha^2 + \beta^i \beta_i & \beta_b \\[2mm] \beta_a & \gamma_{ab} \end{bmatrix}
$$
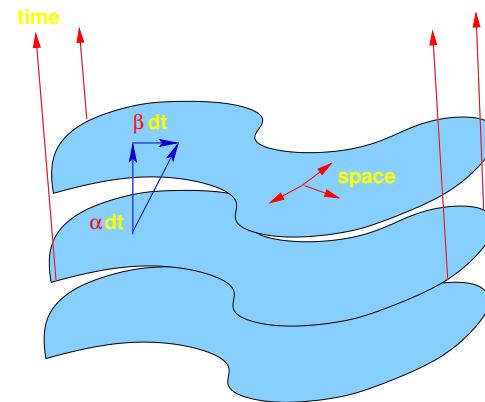
where γ_{ab} is the 3-metric in the slice, α is the lapse (relating the time coordinates between two slices) and β^a is the shift (relating the space coordinates between two slices).

As a result, γ_{ab}, K_{ab} are *dynamical variables*, while α, β^a are *gauge variables*.

6.4 ADM equations - standard form

4D vacuum Einstein equations (10):

$$^{(4)}R_{\mu\nu} - \frac{1}{2}g_{\mu\nu}\,^{(4)}R = 0$$

Evolution equations (6+6):

$$\partial_t \gamma_{ab} = -2\alpha K_{ab} + \mathcal{L}_\beta \gamma_{ab}$$

$$\partial_t K_{ab} = -\nabla_a \nabla_b \alpha + \alpha(R_{ab} + KK_{ab} - 2K_{ai}K^i{}_b) + \mathcal{L}_\beta K_{ab}$$

Constraints (1+3):

$$\mathcal{H} = R + K^2 - K_{ij}K^{ij} = 0 \quad \text{(Hamiltonian)}$$

$$\mathcal{M}_a = \nabla^i(K_{ai} - \gamma_{ai}K) = 0 \quad \text{(Momentum)}$$

Note that the $\mathcal{L}_\beta$ is the Lie derivative along the shift vector and that Ricci tensor R_{ab} is given by second spatial derivatives of the 3-metric γ_{ab}. As a result, this is *not* a first order system.

6.5 Singularity avoiding slicings
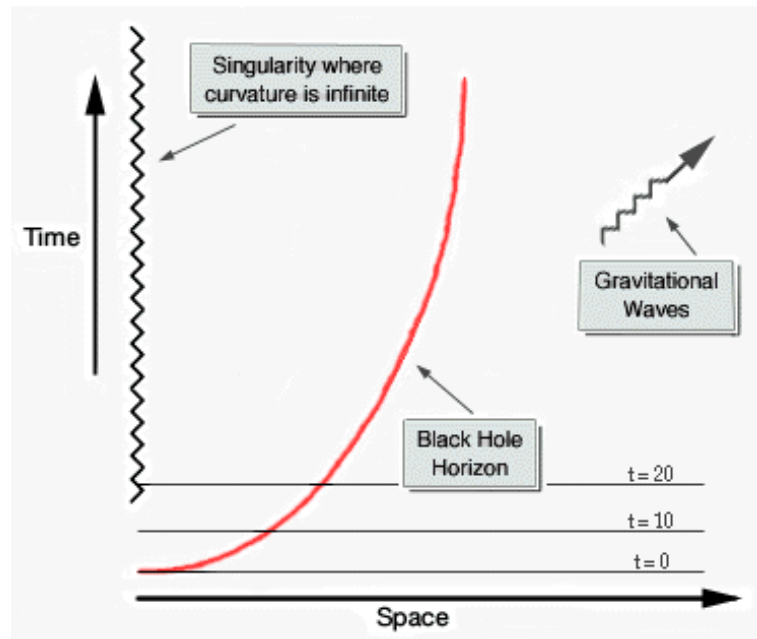
geodesic slicing

$$\alpha = 1$$
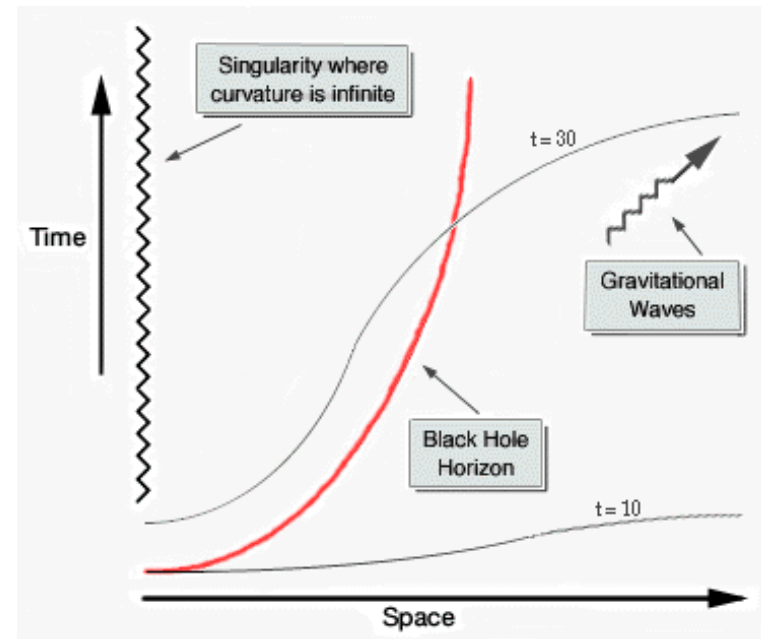
maximal slicing

$$K = 0 \rightarrow -\nabla^i \nabla_i \alpha + \alpha(\tilde{A}_{ij}\tilde{A}^{ij} + \tfrac{1}{3}K^2) + \mathcal{L}_\beta K$$

The geodesic slicing soon "hits" the singularity. However, the maximal slicing may suffer of *slice stretching*, i.e. exponential growth of maxima in the metric at the lapse shoulder.

6.6   Shift conditions

Smarr-York (1978) proposed a shift based on minimizing changes in the metric during evolution.
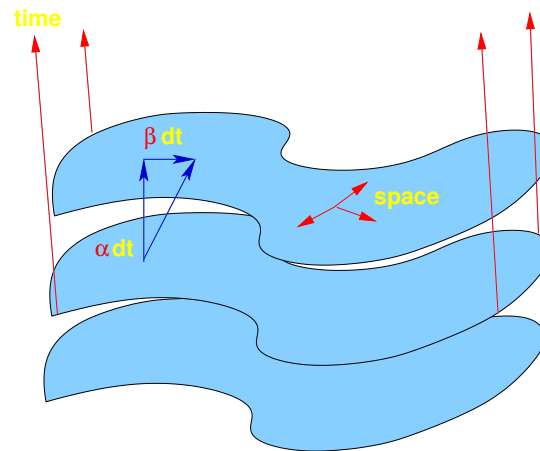
Define:

$$\Theta_{ab} = \tfrac{1}{2} \perp \mathcal{L}_t \tilde{\gamma}_{ab} \qquad \text{(strain tensor)}$$

$$\Sigma_{ab} = \Theta_{ab} - \tfrac{1}{3} \tilde{\gamma}_{ab} \Theta^i{}_i \quad \text{(distortion tensor)}$$

Minimizing $\Sigma_{ij}\Sigma^{ij}$ under changes of β^a leads to the *"minimal distortion shift"*

$$\nabla^i\nabla_i\beta^a + \frac{1}{3}\nabla^a\nabla_i\beta^i + R^a{}_i\beta^i - 2(K^{ai} - \frac{1}{3}\gamma^{ai}K)\nabla_i\alpha = 0$$

6.7 Singularity Excision

The region of the grid inside the event horizon is causally disconnected from the region outside. In principle, the excised region inside the horizon should not influence the evolution outside; in practice it can via gauge-modes.

excision boundary   horizon
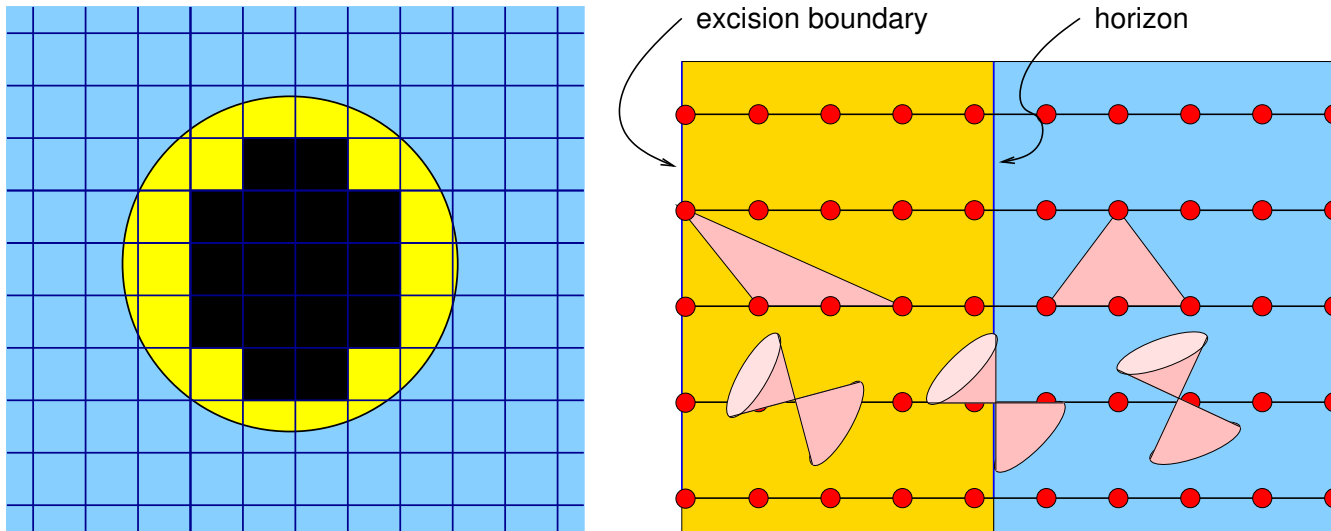
We can cut a region from the grid inside the horizon and remove the singularity (Figs. by D. Pollney). The boundary condition should not influence the evolution outside.

6.8 Relativistic Hydrodynamics Equations

The hydrodynamical equations are given by the local conservation of baryon number and of energy-momentum

$$\nabla_\mu J^\mu = \nabla_\mu(\rho u^\mu), \tag{58}$$

and

$$\nabla_\mu T^{\mu\nu} = \nabla_\mu(\rho h u^\mu u^\nu + p g^{\mu\nu}), \tag{59}$$

respectively, where ρ is the rest-mass density, p the pressure, h the specific enthalpy, and $g_{\mu\nu}$ the metric components. The usual thermodynamic expressions relating e and p to the specific enthalpy h and to the specific internal energy ϵ of the fluid are

$$e = \rho(1 + \epsilon), \tag{60}$$

$$h = 1 + \epsilon + \frac{p}{\rho}. \tag{61}$$

An equation of state $p = p(\rho, \varepsilon)$ closes the system.

The relativistic Euler equations were recast as a hyperbolic system of conservation laws. In particular, the Jacobian matrix of the system was obtained explicitly in terms of suitable *conserved variables*. As a result, this formulation allows the spectral decomposition of the system and, therefore, the application of all of those Godunov type methods involving approximate Riemann solvers where this information is required.

Using the $3 + 1$ decomposition of the metric, all measurements can be referred to an Eulerian observer $\mathbf{n}$ at rest in the spacelike slice. In particular, the components of the three velocity of the fluid measured by $\mathbf{n}$ are given by

$$v^i = \frac{\mathbf{P} \cdot \mathbf{u}}{-\mathbf{n} \cdot \mathbf{u}} = \frac{u^i}{\alpha u^t} + \frac{\beta^i}{\alpha}, \tag{62}$$

where $\mathbf{P}$ is the projector orthogonal to $\mathbf{u}$, $W \equiv -(\mathbf{u} \cdot \mathbf{n}) = \alpha u^t$ is the Lorentz factor, satis-

fying $W = (1 - v^2)^{-1/2}$, with $v^2 = \gamma_{ij} v^i v^j$. We now introduce suitable *"conserved"* variables allowing for a conservative formulation of the general relativistic hydrodynamic equations. These are not the ordinary fluid, or *"primitive"*, variables $\mathbf{w} = (\rho, v_i, \epsilon)$, but rather the quantities $\mathbf{U}(\mathbf{w}) = (D, S_j, \tau)$, with

$$D = \rho W \,,$$

$$S_j = \rho h W^2 v_j \,,$$

$$\tau = \rho h W^2 - p - D \,. \tag{63}$$

Here D, S_j and E are the rest mass density, the momentum in the j-direction and the total energy density, respectively, as measured by the Eulerian observer. As a result, the fundamental system in quasi-conservation form reads

$$\frac{1}{\sqrt{-g}} \left(\frac{\partial \sqrt{\gamma} \mathbf{U}(\mathbf{w})}{\partial x^0} + \frac{\partial \sqrt{-g} \mathbf{F}^i(\mathbf{w})}{\partial x^i} \right) = \mathbf{s}(\mathbf{w}), \tag{64}$$

where $g \equiv \det(g_{\mu\nu})$ and $\sqrt{-g} = \alpha\sqrt{\gamma}$ ($\gamma \equiv \det(\gamma_{ij})$). The fluxes $\mathbf{F}^i(\mathbf{w})$ and the source terms $\mathbf{s}(\mathbf{w})$ in (64) take the explicit form

$$\mathbf{F}^i(\mathbf{w}) = \left(D\left(v^i - \frac{\beta^i}{\alpha}\right), S_j\left(v^i - \frac{\beta^i}{\alpha}\right) + p\delta^i_j, \tau\left(v^i - \frac{\beta^i}{\alpha}\right) + pv^i \right), \tag{65}$$

and

$$\mathbf{s}(\mathbf{w}) = \left(0, T^{\mu\nu}\left(\frac{\partial g_{\nu j}}{\partial x^\mu} - \Gamma^\delta_{\nu\mu}g_{\delta j}\right), \alpha\left(T^{\mu 0}\frac{\partial \ln\alpha}{\partial x^\mu} - T^{\mu\nu}\Gamma^0_{\nu\mu}\right) \right), \tag{66}$$

respectively, where the $\Gamma^{\mu\nu}_\beta$'s are the Christoffel symbols of the given metric. Note that the presence of the source terms $\mathbf{s}(\mathbf{w})$ does not prevent the application of conservative methods, since the sources do not include gradients of the conserved variables and are jsut related to the curvature of the metric.

7 Initial Data
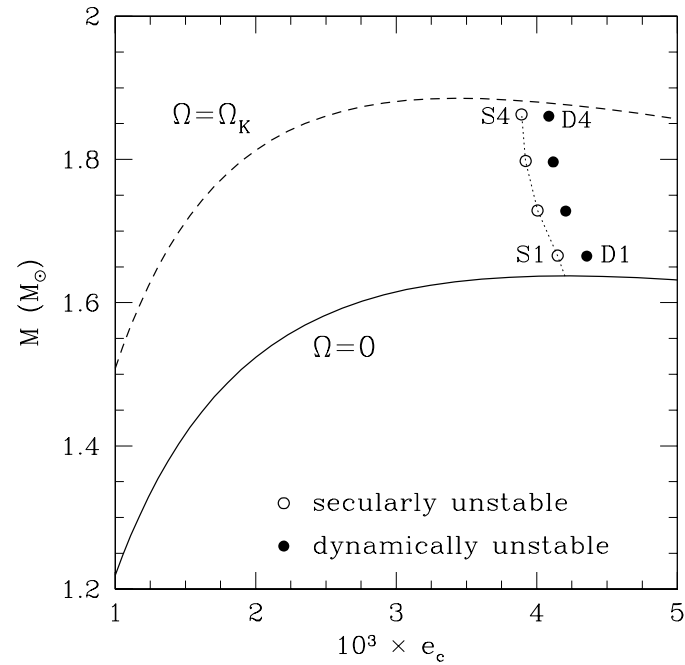
Figure 4: Gravitational mass shown as a function of the central energy density for equilibrium models constructed with the polytropic equation of state ($\Gamma = 2$, $K_{\text{ID}} = 100$). The solid, dashed and dotted lines correspond to the sequence of nonrotating models, the sequence of models rotating at the mass-shedding limit and the sequence of models that are at the onset of the secular instability to axisymmetric perturbations.

7.1 Slowly Rotating Stars
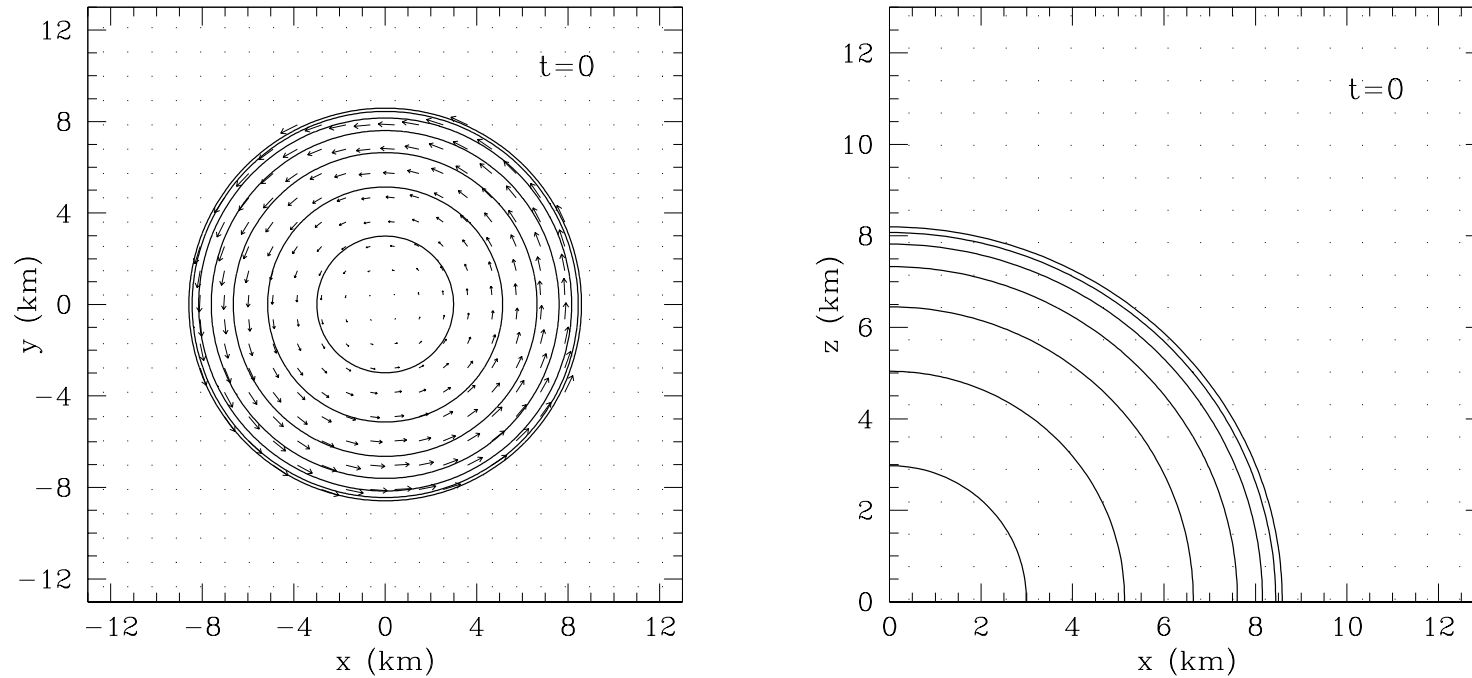
Figure 5: Collapse sequence for the slowly rotating model D1. Different panels refer to different snapshots during the collapse and show the isocontours of the rest-mass density and velocity field in the (x, y) plane (left column) and in the (x, z) plane (right column), respectively.

Initially, no radial motion is present and the star is almost spherical.
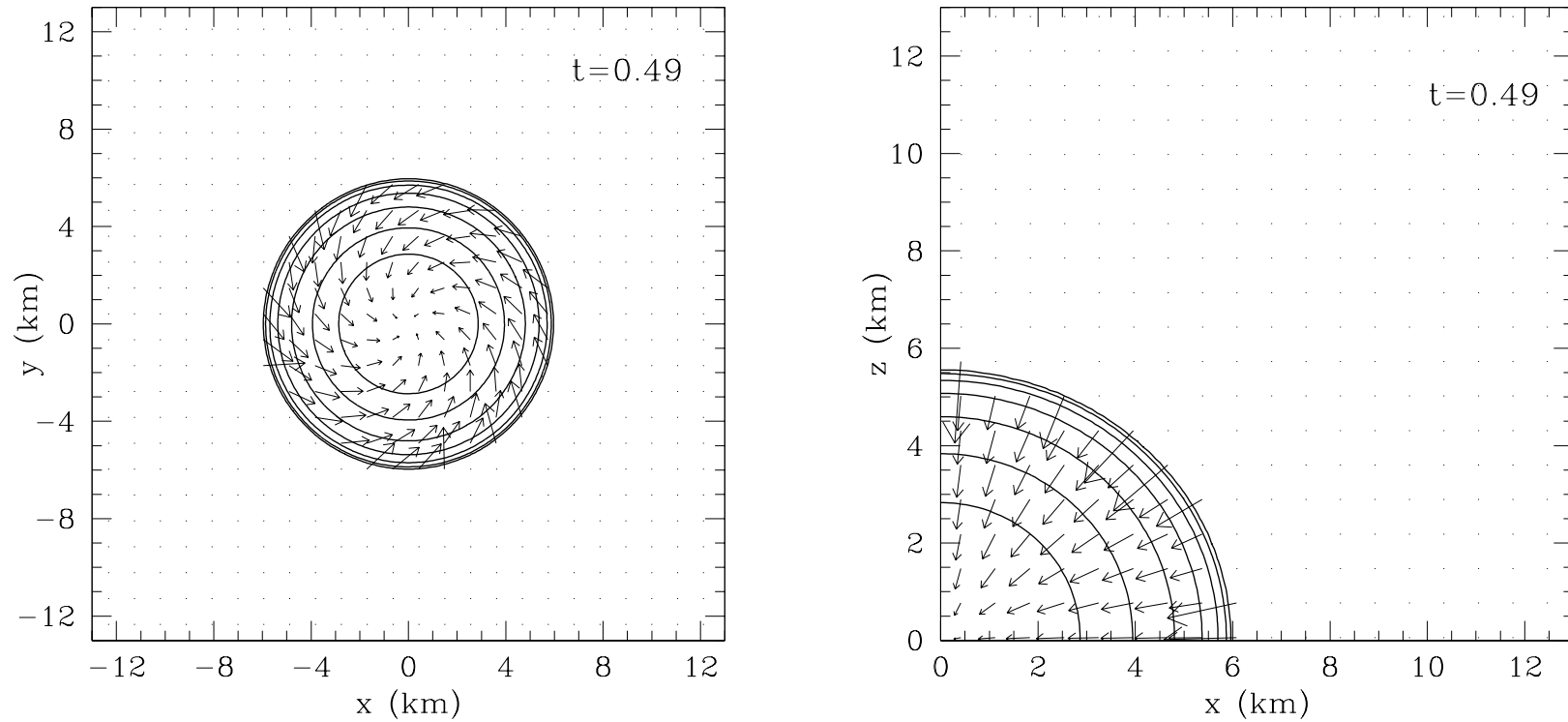
Figure 6: Time = 0.49 ms.

During the collapse the star increases its compactness and the matter is compressed to larger pressures, the velocity field acquires a radial component.
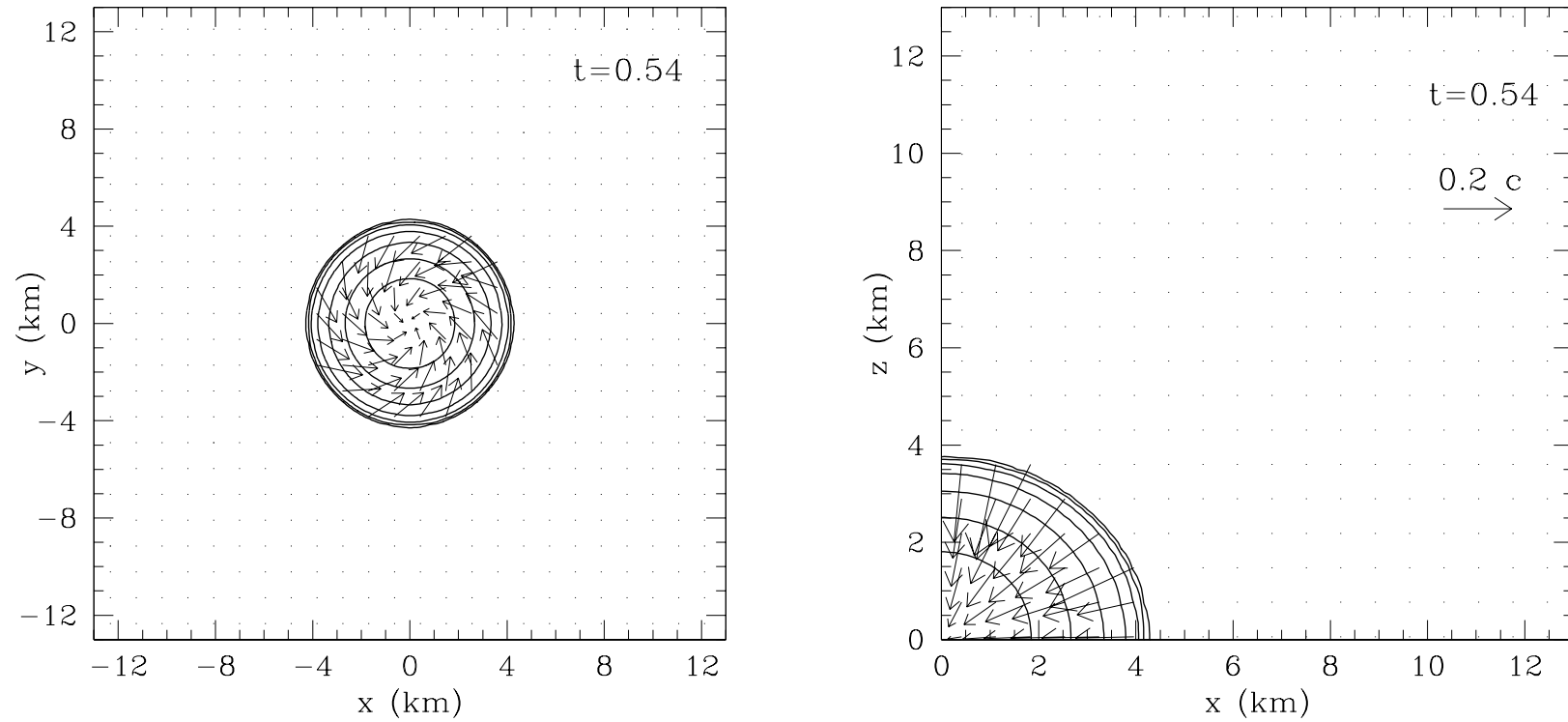
Figure 7: Time = 0.54 ms.

The collapse speeds up and relativistic radial velocities are reached rapidly.
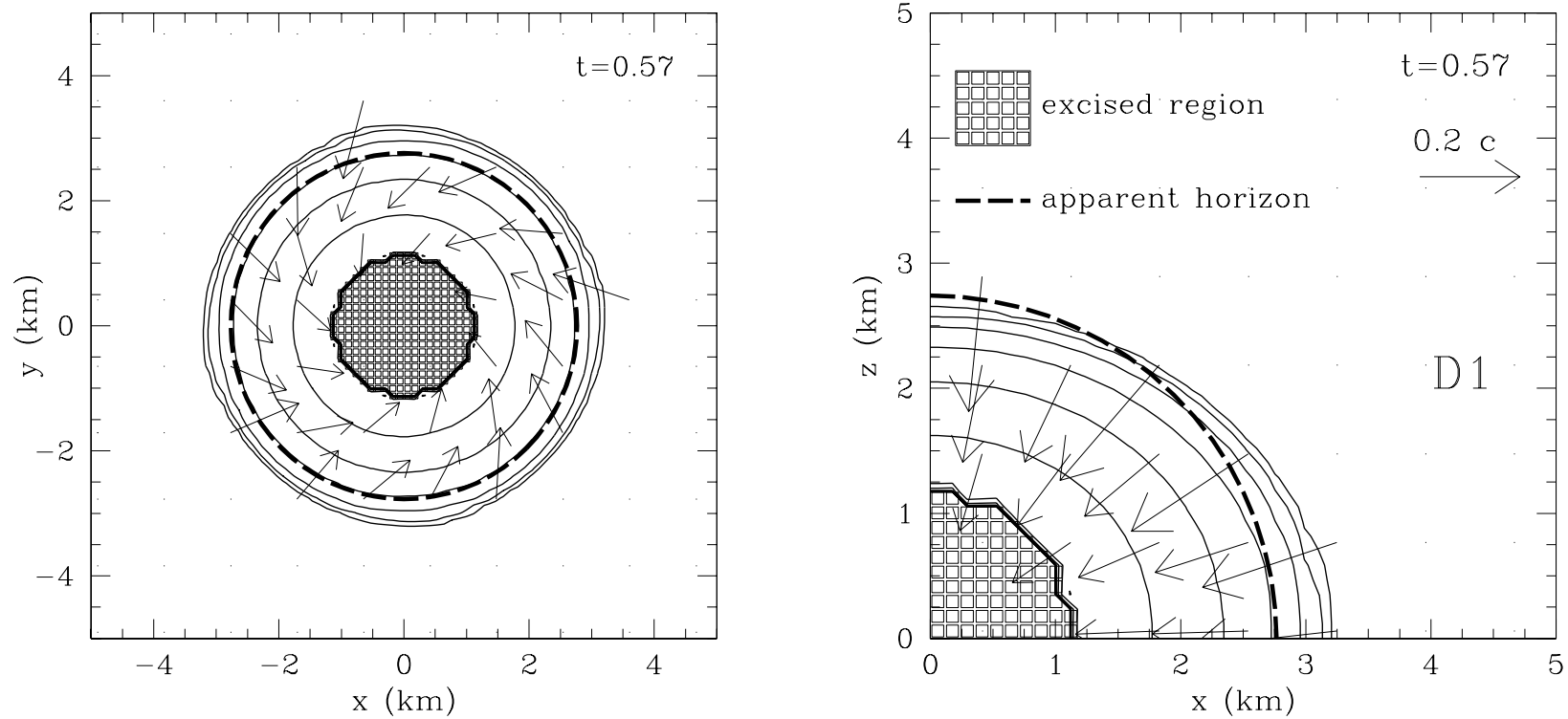
Figure 8: Time = 0.57 ms: an apparent horizon has just been formed.

An apparent horizon is found and the portion of the computational domain containing the singularity is excised.

7.2   Rapidly Rotating Stars
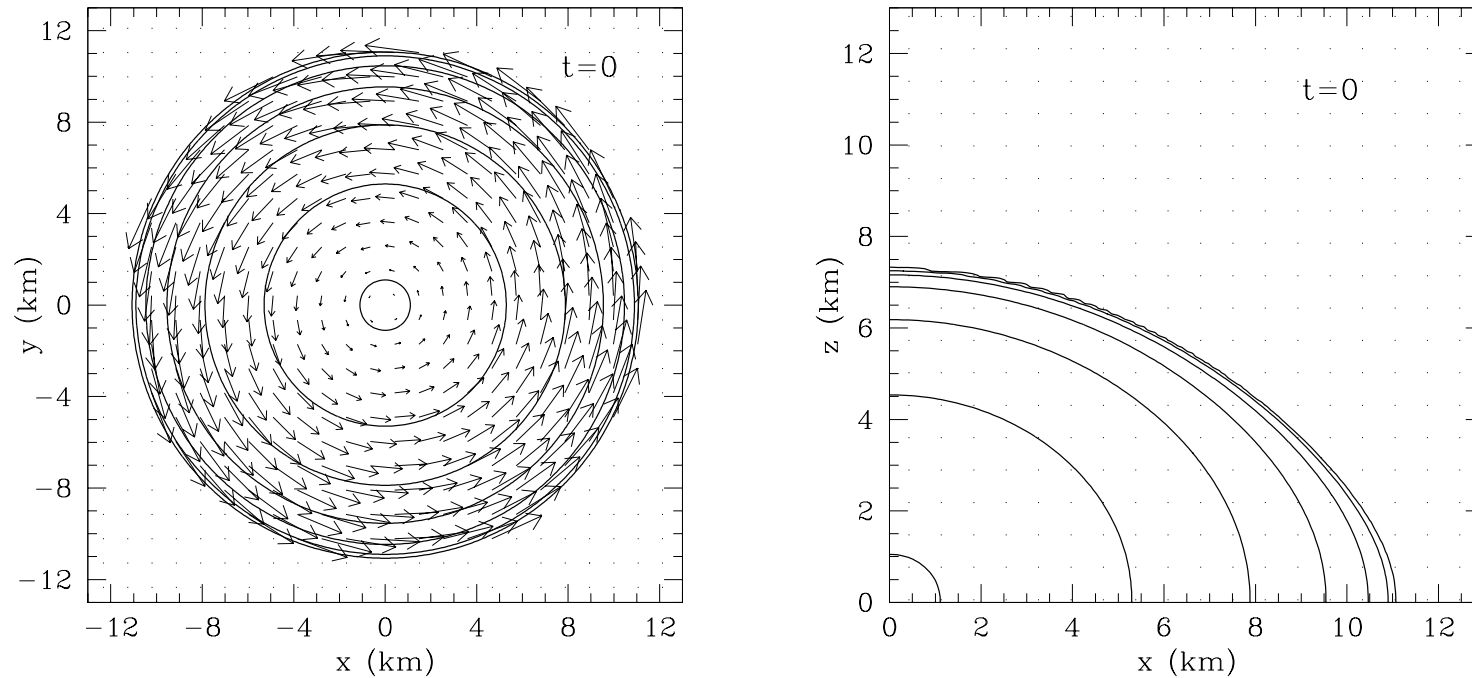
Figure 9: Collapse sequence for the rapidly rotating model D4. The conventions used in these panels are the same as in Fig. 5, which can be used for a comparison with the collapse of a slowly rotating model.

Initially, no radial motion is present and the star is considerably flattened with axis ratio $r_p/r_e = 0.65$.
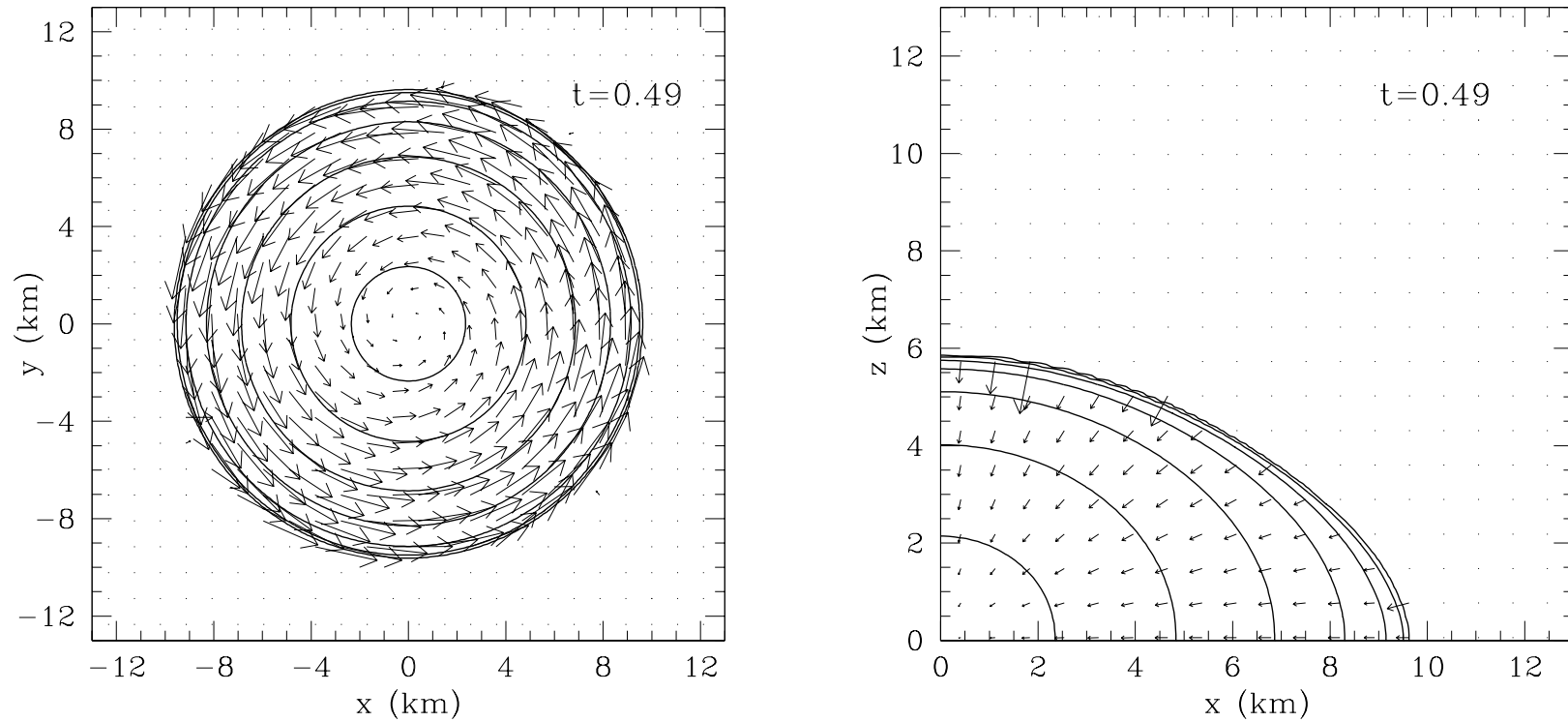
Figure 10: Time = 0.49 ms.

The parts of the star around the rotation axis that are experiencing smaller centrifugal forces collapse more promptly and, as a result, the configuration increases its oblateness.
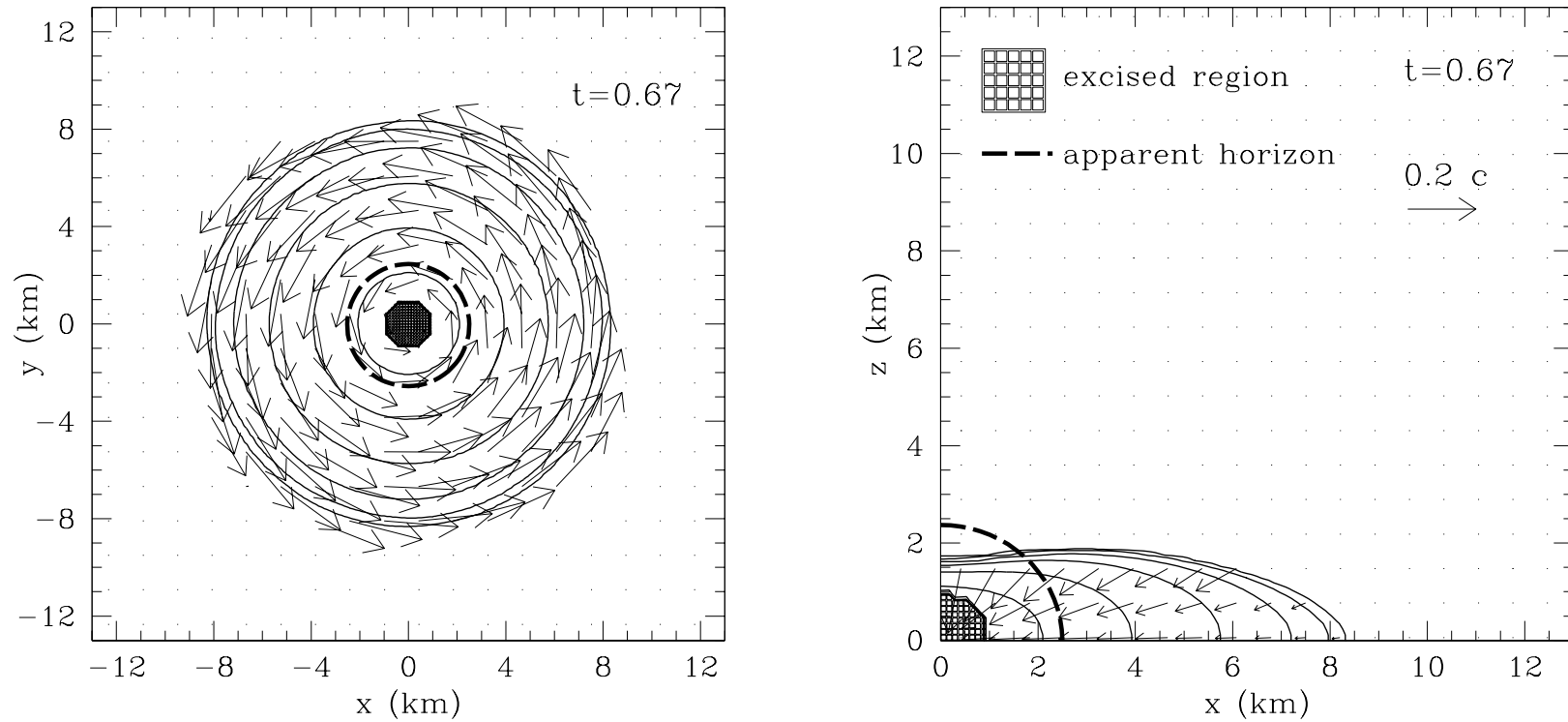
Figure 11: Time = 0.67 ms: an apparent horizon has just been formed.

The star has flattened considerably, the matter near the rotation axis has fallen inside the apparent horizon, but a disc of low-density matter has formed orbiting at $\sim 0.2c$.
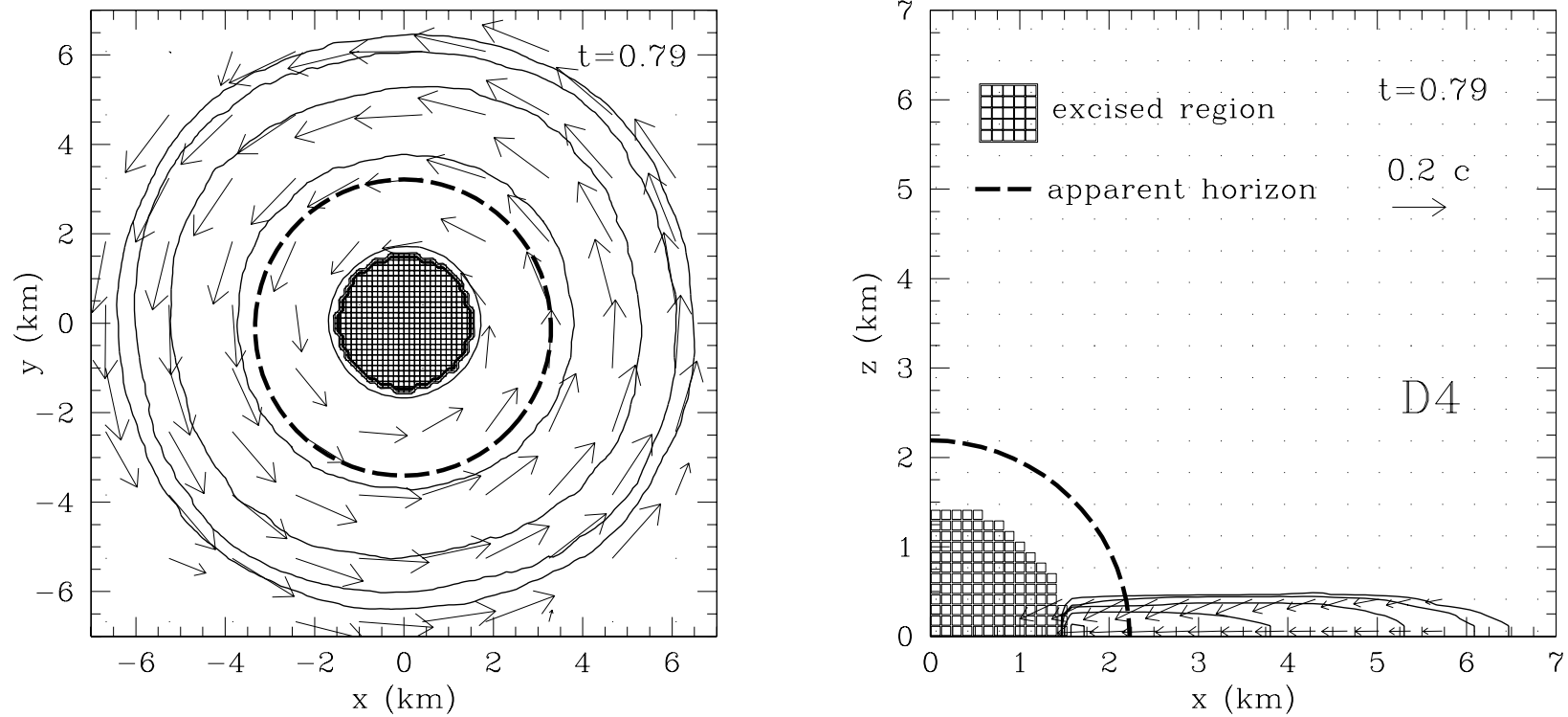
Figure 12: Time = 0.79 ms: the disc is unstable and is rapidly accreted onto the black hole.

The disc outside the apparent horizon is *not* dynamically stable and it rapidly accretes onto the black hole. Animations can be found at `www.sissa.it/~rezzolla/WhiskyI`.

8 Non-spherical Fluid Collapse: Trapped Surfaces

As mentioned above, the dynamics of trapped surfaces in a perfect fluid collapse is similar to the one in the OS collapse continues to hold also in the case of the collapse of a perfect fluid. The first important difference is that the apparent horizon is produced "earlier", i.e. before the stellar surface reaches $R = 2M$ but can, because of the fluid compression, be formed also earlier. The second difference appears in multidimensional calculations and is caused by the rotation of initial data, which gives rise to both apparent and event horizons that are not spheres but, oblate spheroids, i.e. with a polar proper circumference which is smaller than the corresponding equatorial one.
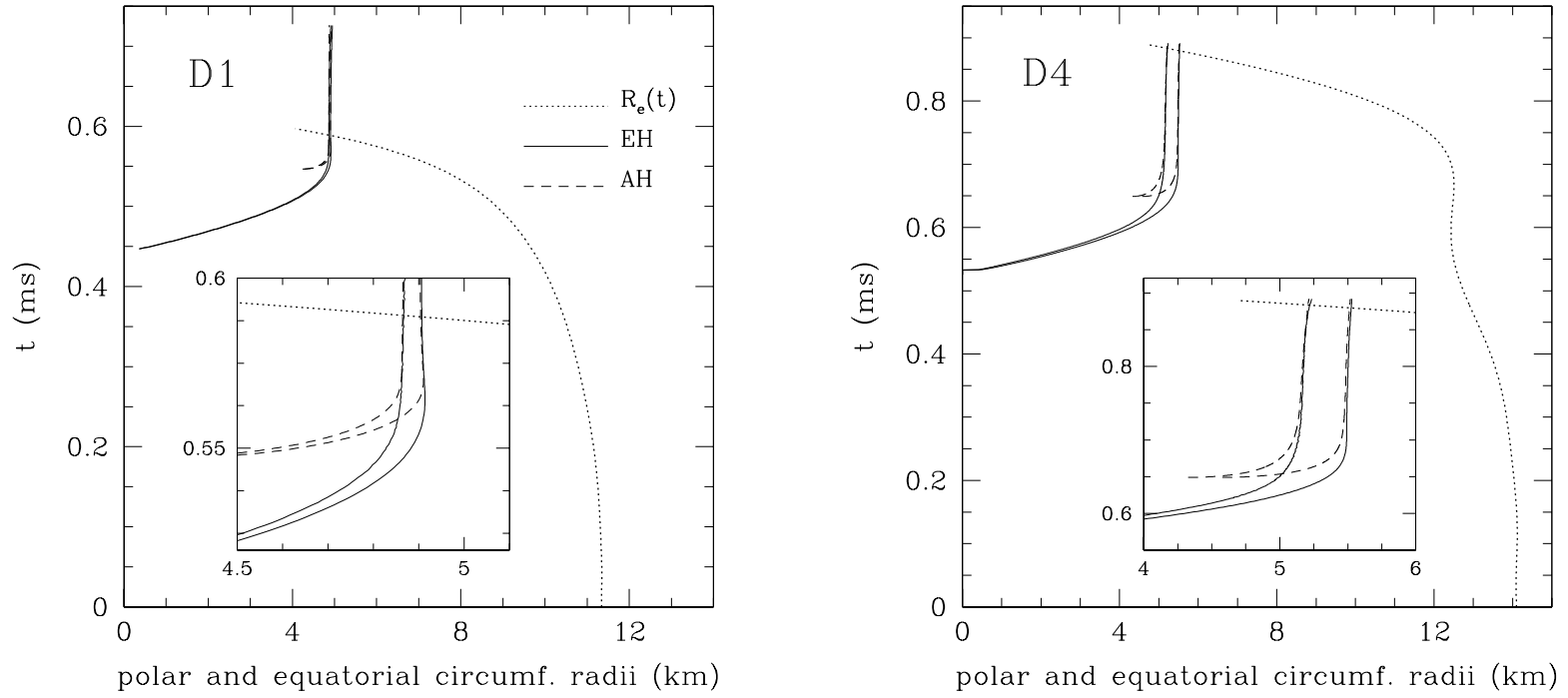
Figure 13: Solid, dashed and dotted lines represent the worldlines of the circumferential radii of the event horizon, of the apparent horizon and of the stellar surface, respectively. Note that for the horizons we plot both the equatorial and the polar circumferential radii.

9 Some energy estimates from numerical simulations

So far, the numerical investigation of the energy loss to gravitational waves has been discussed in two different works only. The first one, by Stark and Piran (1985) was restricted to axisymmetric configurations and computed the gravitational wave emission from the collapse of rapidly rotating stars to black holes. While the initial data was rather <u>unrealistic</u> and with a <u>large error</u> in the constraint equations, these calculations are probably the most accurate to-date because of the large spatial resolution allowed by a 2D simulation.

The recent calculations by Baiotti et al. (2004) have computed the energy loss to gravitational waves. Although this is the <u>first estimate in 3D</u>, it still has a rather large truncation error.

The energy estimates in the two cases are:

- Stark and Piran (1985): 2D, spherical coordinates, unrealistic initial data

$$\Delta E / M \simeq 1.4 \times 10^{-4} \ (J/M^2)^4 \quad \text{for} \quad (J/M^2) \lesssim 0.5$$

- Baiotti, Rezzolla et al. (1985): 3D, Cartesian coordinates, realistic initial data

$$\Delta E / M \simeq 5.0 \times 10^{-3} \quad \text{for} \quad (J/M^2) \ll 1$$

$$\Delta E / M \simeq 1.0 \times 10^{-2} \quad \text{for} \quad (J/M^2) \sim 0.5$$

where it is important to underline that the in the 3D simulations, the low resolution allows

to determine upper limits only, which are entirely due to the large truncation error. It is

likely that the estimates will converge to similar values once resolutions comparable to the

2D simulations will be reached also in 3D simulations.

References

[1] C. W. Misner, K. S. Thorne and J. A. Wheeler, *"Gravitation"*, Freeman, NY (1974)

[2] B. F. Schutz, *"An Introduction to General Relativity"*, Cambrige Univ. Press, Cambridge UK (1984)

[3] R. d'Inverno, *"Introducing Einstein's Relativity"*, Oxford Univ. Press, Oxford UK (1990)

[4] S. Chandrasekhar, *"The Mathematical Theory of Black Holes"*, Oxford Univ. Press, Oxford UK (1992)

[5] R. F. Stark and T. Piran, Phys. Rev. Lett. 55, 891 (1985).

[6] L. Baiotti, I. Hawke, P. J. Montero, F. Löffler, L. Rezzolla, N. Stergioulas, J. A. Font, and Ed Seidel `gr-qc/0403029` (2004)